Effective hydraulic properties of 3D virtual stony soils identified by inverse modeling

Mahyar Naseri*, Sascha C. Iden, and Wolfgang Durner

Division of Soil Science and Soil Physics, Institute of Geoecology, Technische Universität Braunschweig, Germany

**Corresponding author:* m.naseri@tu-bs.de, Langer Kamp 19c, 38106 Braunschweig, Germany

s.iden@tu-bs.de, Langer Kamp 19c, 38106 Braunschweig, Germany

w.durner@tu-bs.de, Langer Kamp 19c, 38106 Braunschweig, Germany

Core Ideas

- Virtual stony soils with different rock fragment contents were generated in 3D using the Hydrus 2D/3D software.
- Evaporation experiments and unit-gradient experiments were numerically simulated.
- We used inverse modelling with the Richards equation to identify effective hydraulic properties of virtual stony soils.
- The identified hydraulic properties were used to evaluate the scaling models of calculating hydraulic properties of stony soils.

Keywords

Soil hydraulic properties, water retention curve, hydraulic conductivity, stony soil, inverse modeling, Hydrus 2D/3D

Abstract

Stony soils that have a considerable amount of rock fragments (RF) are widespread around the world. However, experiments to determine effective hydraulic properties of stony soils (SHP), i.e. the water retention curve (WRC) and hydraulic conductivity curve (HCC), are challenging. Installation of measurement devices and sensors in these soils is difficult and the data are less reliable because of their high local heterogeneity. Therefore, effective properties of stony soils especially in unsaturated hydraulic conditions are still not well understood. An alternative approach to

evaluate the SHP of these systems with internal structural heterogeneity is numerical simulation. We used the Hydrus 2D/3D software to create virtual stony soils in 3D and simulate water flow for different volumetric fractions of RF, f. Stony soils with different values of f from 11 to 37 % were created by placing impermeable spheres as rock fragments in a sandy loam soil. Time series of local pressure heads in various depths, mean water contents, and fluxes across the upper boundary were generated in a virtual evaporation experiment. Additionally, a multi-step unit gradient simulation was applied to determine effective values of hydraulic conductivity near saturation up to $pF = 2$. The generated data were evaluated by inverse modeling, assuming a homogeneous system, and the effective hydraulic properties were identified. The effective properties were compared with predictions from available scaling models of SHP for different values of f. Our results showed that scaling the WRC of the background soil based on only the value of f gives acceptable results in the case of impermeable RF. However, the reduction of conductivity could not be simply scaled by the value of f. Predictions were highly improved by applying the Novák, Maxwell, and GEM models to scale the HCC. The Maxwell model matched the numerically identified HCC best.

1. Introduction

Stony soils are soils with a considerable amount of rock fragments (RF) and are widespread in mountainous and forested watersheds around the world (Ballabio et al., 2016; Novák and Hlaváčiková, 2019). RF in soil are particles with an effective diameter of larger than 2 mm (Tetegan et al., 2015; Zhang et. al., 2016). Their existence in soil influences the two constitutive soil water relationships known as soil hydraulic properties (SHP) i.e. water retention curve (WRC), and hydraulic conductivity curve (HCC) (Russo, 1988; Durner and Flühler, 2006). The accurate identification of SHP is a prerequisite for adequate prediction of water flow in soil with the Richards equation (Farthing and Ogden, 2017; Haghverdi et al., 2018). The SHP depend on soil texture and structure (Kutilek, 2004; Lehmann et al., 2020), and are influenced by the presence of RF in soil. It is generally accepted that RF decrease the water storage capacity of soils and its effective unsaturated hydraulic conductivity. In contrast, the formation of macropores in the vicinity of embedded RF may lead to an increase in saturated hydraulic conductivity. While experimental evidence and theoretical analyses show that the volumetric fraction of RF, f (v/v), has the highest influence on effective SHP of stony soil, the effect of other characteristics of RF such as their porosity, shape, size, arrangement, and orientation towards flow is less clear (Hlaváčiková and Novák, 2014; Hlaváčiková et al., 2016; Naseri et al., 2020). Up to the present, two approaches have been dominant in identifying the hydraulic behavior of stony soils: I) Experimental setups with the aim of measuring SHP of stony soils in the field or in controlled systems

in the laboratory (Cousin et al., 2003; Dann et al., 2009; Grath et al., 2015; Beckers et al., 2016, Naseri et al., 2019), and II) Development of empirical, physical or physico-empirical approaches to scale hydraulic properties of background soil based on the value of f and characteristics of RF (Novák et al., 2011; Naseri et al., 2020). These two approaches have some systematic limitations that restrict their applications in investigating the hydraulic behavior of stony soils. Installation of sensors and measurement instruments in the stony soils are technically demanding (Cousin et al., 2003; Verbist et al., 2013, Coppola et al., 2013; Stevenson et al., 2021), undisturbed sampling is laborious (Ponder and Alley, 1997), relatively larger samples are required (Germer and Braun, 2015), and the measured data might be more inconsistent due to the higher local heterogeneity of such soils (Baetens et al., 2009; Corwin and Lesch, 2005). Furthermore, some of the available scaling models to obtain effective SHP are conceptually oversimplified and they exclusively consider the value of f as the only input parameter (Bouwer and Rice, 1984; Ravina and Magier, 1984). Additionally, they assume impermeable RF and are proposed mainly for saturated flow conditions. These scaling models need a systematic verification under variably-saturated conditions using experimental data or 3D simulations. Some reviews of these models and their evaluation are available in the literature (Brakensiek et al., 1986; Novák et al., 2011; Beckers et al., 2016; Naseri et al., 2019).

Hlaváčiková and Novák (2014) proposed a model to scale the HCC of the background soil, parametrized with the van Genuchten–Mualem (van Genuchten, 1980) model, using the model of Bower and Rice (1984). Hlaváčiková et al., (2018) used the water content of RF as input parameter to scale the WRC of the background soil. Naseri et al. (2019) used the simplified evaporation method (Peters et al., 2015) to determine experimentally the effective SHP of small soil samples containing various amounts of RF. Their study criticizes the application of the scaling models developed for saturated stony soils to unsaturated conditions and emphasizes the need to develop approaches that consider more characteristics of the RF to calculate SHP of the stony soils.

Recent advancements in computational hydrology and computing power suggest the numerical simulation of soil water dynamics as a promising alternative to the measurement of effective SHP of heterogeneous soils (Durner et al., 2008; Lai and Ren, 2016; Radcliffe and Šimůnek, 2018). Numerical simulations have several advantages. They do not demand strict experimental setups, are repeatable under a variety of initial and boundary conditions, and in contrast to the laboratory experiments, space and time scales are not restrictive factors in the simulations. These assets have made them a favorable tool in water and solute transport modeling in heterogeneous soils (Abbasi et al., 2003;

Šimůnek et al., 2016). However, with few exceptions, heterogeneous soils like stony soils have been simulated only for simplified cases, i.e., either under fully saturated conditions or with reduced dimensionality, i.e., simulations of stony soils in two spatial dimensions (2D). Novák et al. (2011) calculated effective saturated hydraulic conductivity (K_s) of soils containing impermeable RF using steady-state simulations with the software Hydrus 2D which solves the Richards equation in two spatial dimensions. They derived a linear relationship between K_s of stony soils and f. Hlaváčiková et al. (2016) simulated different shapes and orientations of RF in Hydrus 2D to obtain the effective K_s of the virtual stony soils. Beckers et al. (2016) used Hydrus 2D simulations to extend the investigations towards the impact of f, shape, and size of RF on the HCC. They also identified effective SHP of a clay stony soil using laboratory evaporation experiments for f values up to 20 % (v/v).

The inverse modeling approach has been applied to identify effective hydraulic properties of soils in laboratory experiments (Ciollaro and Romano, 1995; Hopmans et al., 2002; Nasta et al., 2011), in lysimeters and field (Abbaspour et al., 1999; Abbaspour et al., 2000), virtual lysimeters with internal textural heterogeneity (Durner et al., 2008; Schelle et al., 2013), and WRC of stony soils through field infiltration experiments (Baetens et al., 2009). Although theoretical studies and laboratory investigations on packed samples are insufficient to understand fully the hydraulic processes in stony soils, they do lead the way to the improvement and validation of effective models and their application at the field and even larger scales. Inverse modeling is arguably the best approach to achieve these aims because it allows to validate effective models using process modeling. Our aim in this study was to investigate the application of inverse modeling to identify the effective SHP of 3D virtual stony soils and to explore its applicability to these soil systems as an example of internal structural heterogeneity. We were interested in answering the following questions:

i) Is it possible to describe the dynamics in the heterogeneous 3D system with the 1D Richards equation assuming a homogeneous soil?

ii) If so, what are the effective SHP of stony soils and how are they related to the SHP of the background soil?

To answer these questions we conducted forward simulations of water movement in 3D using the Richards equation as variably-saturated flow model. We created stony soils by embedding voids representing impermeable spherical RF as inclusions into a homogeneous background soil. Then we simulated transient evaporation experiments and stepwise steady-state, unit-gradient infiltration experiments in 3D. The generated data were used as an input to a 1D inverse

model to obtain the effective SHP of stony soils, and these properties were used to evaluate and compare the available scaling models of SHP for stony soils.

2. Materials and methods

2.1. Simulation model

The Hydrus 2D/3D software was used to generate virtual stony soils and simulate the water flow in the created three-dimensional geometries. Water flow in Hydrus 2D/3D is modelled by the Richards equation (Šimůnek et al., 2006; 2008), which is the standard model for variably-saturated water flow in porous media. The Hydrus 2D/3D software solves the mixed form of the Richards equation numerically using the finite-element method and an implicit scheme in time (Celia et al., 1990; Šimůnek et al., 2008; 2016; Radcliffe and Šimůnek, 2018). The three-dimensional form of the Richards equation under isothermal conditions, without sinks/sources, and assuming an isotropic hydraulic conductivity is:

$$\frac{\partial \theta}{\partial t} = \frac{\partial}{\partial x}\left[K(h)\left(\frac{\partial h}{\partial x}\right)\right] + \frac{\partial}{\partial y}\left[K(h)\left(\frac{\partial h}{\partial y}\right)\right] + \frac{\partial}{\partial z}\left[K(h)\left(\frac{\partial h}{\partial z} + 1\right)\right] \quad (1)$$

where θ is the volumetric water content (cm^3 cm^{-3}), t is time (s), h is the pressure head (cm), and $K(h)$ is the hydraulic conductivity function (cm d^{-1}). x, and y (cm) are the horizontal Cartesian coordinates, and z (cm) is the vertical coordinate, positive upwards. We used the van Genuchten-Mualem model to parametrize the WRC and HCC (van Genuchten, 1980):

$$S_e(h) = \frac{\theta(h) - \theta_r}{\theta_s - \theta_r} = [1 + (\alpha h)^n]^{-m} \quad (2)$$

and

$$K(h) = K_s S_e^{\tau}\left[1 - \left(1 - S_e^{\frac{1}{m}}\right)^m\right]^2 \quad (3)$$

where θ_s and θ_r are the saturated and residual water contents (cm^3 cm^{-3}), respectively, $S_e(h)$ is the effective saturation (-), α (cm^{-1}) is a shape parameter, n is an empirical parameter related to the pore size distribution (-) and $m = 1 - 1/n$, K_s is the saturated hydraulic conductivity and τ is a tortuosity/connectivity parameter (-).

2.2. 3D geometries representing stony soils

The virtual stony soils in 3D were created by placing spherical inclusions in a background soil. In accordance with real laboratory experiments (not reported here), we generated virtual soil columns as cylinders with a diameter of 16 cm and a height of 10 cm and an total volume of ≈2011 cm^3. The inclusions were considered as voids representing impermeable RF embedded in the background soil. Configurations and characteristics of the created 3D geometries of stony soils are illustrated in Fig. 1. Each spherical inclusion had a diameter of 3.04 cm and a volume of ≈14.7 cm^3. Stony soils with different values of f were created by including different numbers of spherical inclusions in the soil column. A total number of 15, 27, 39, and 51 spherical inclusions in each column led to four volumetric rock fragment contents of 11.0, 19.8, 28.5 and 37.3 % (v/v). Spheres were arranged in the column in three layers. The spheres' centers were in depths of 2.5, 5.0 and 7.5 in the column and each layer was packed with one-third of the total number of intended spheres. Furthermore, observation points at selected nodes of the numerical grid were inserted in each of the three depths of the column (i.e. 2.5, 5.0 and 7.5 cm) in the background soil and not in close vicinity of the inclusions to provide time series of soil water pressure head for the inverse simulations. For the background soil, a homogenous sandy loam soil was considered with the van Genuchten-Mualem model parameters $\theta_s = 0.410$ ($cm^3\ cm^{-3}$), $\theta_r = 0.065$ ($cm^3\ cm^{-3}$), $\alpha = 0.01$ (cm^{-1}), $n = 2.0$ (-), $\tau = 0.5$ (-), and $K_s = 100$ (cm d^{-1}). The targeted mesh size for the different simulations was set to 0.25 cm. The dependency of the numerical solution on the mesh size was tested with some refined meshes and negligible differences in the results were obtained for different mesh sizes.

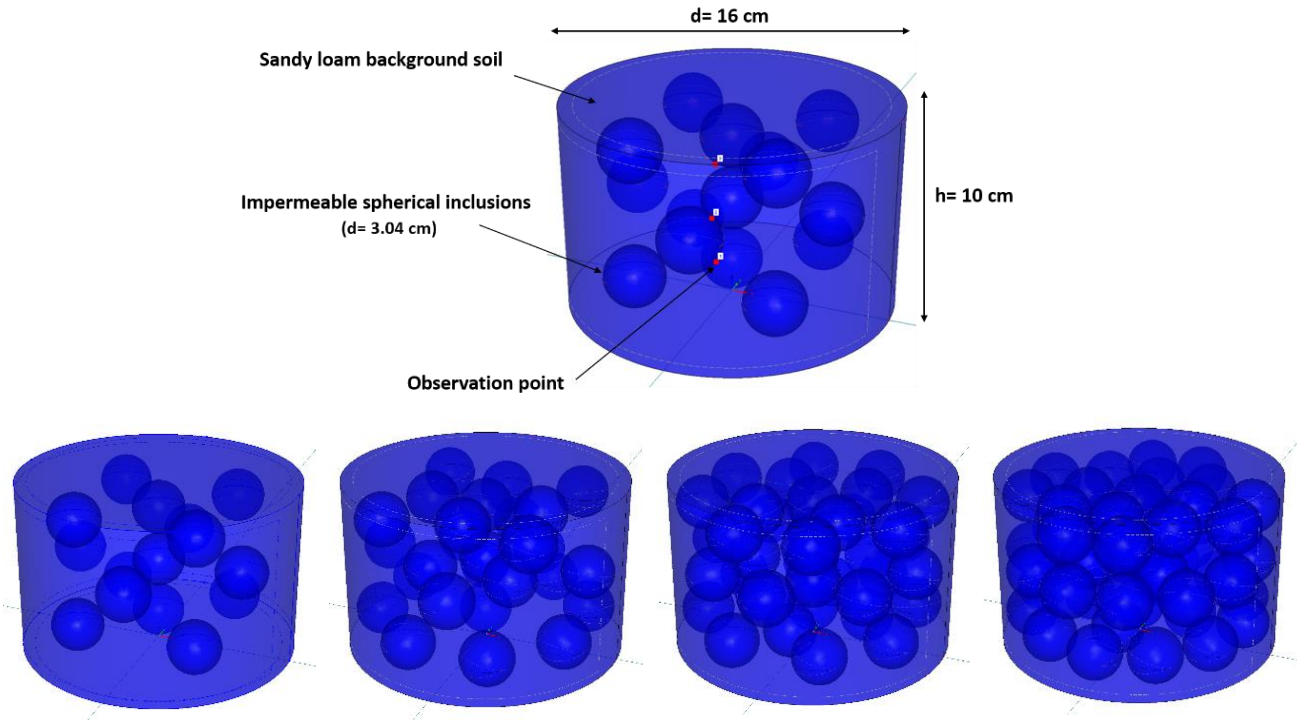

Figure 1: Visualization of the generated stony soils in 3D, including the dimension of rock fragments and soil cylinder and location of the observation points (top). Bottom row shows rock fragment contents of 11.0, 19.8, 28.5 and 37.3 %, from left to right.

2.3. Forward simulations

We simulated evaporation (EVA) (Peters and Durner, 2008) and multistep unit gradient (MSUG) experiments (Sarkar et al., 2019). For EVA, a linear distribution of pressure head (-2.5 cm top, +7.5 cm bottom) was used as the initial condition. The boundary conditions were no-flux at the bottom and atmospheric with a constant potential evaporation rate of 0.6 (cm d^{-1}) and zero precipitation at the top. The EVA experiments were simulated for 10 days and the time series of pressure heads at each observation point, the initial volumetric water content and the cumulative evaporation and evaporation rate were collected for later use in the inverse simulations.

In the virtual MSUG experiment, the soil column was initially fully saturated with a constant pressure head of 0 cm. A sequence of step-wise decreasing constant pressure heads was assigned to the upper and lower boundaries of the column. The duration of the virtual MSUG experiment was 100 days and the pressure head in the upper and lower boundaries was simultaneously decreased stepwise to a pressure head of -100 cm. The applied pressure heads h_i were 0, -1, -3, -10, -20, -30, -60, and -100 cm, respectively. Time steps were chosen such that a steady-state flow condition was reached for each pressure step, indicated by identical water fluxes at the top (inflow) and bottom (outflow)

boundaries and constant pressure heads at the observation points. The hydraulic conductivities at the respective pressure heads h_i data were calculated by dividing the steady-state water flux rates ($cm^3\ d^{-1}$) by the total surficial area of the soil column ($\approx 202\ cm^2$).

The converging and diverging flow field around obstacles produces even under unit gradient conditions spatially different pressure heads, and as opposed to saturated conditions, these different pressure heads are under unsaturated conditions associated with different water saturations and different local hydraulic conductivities. We were interested in whether and to what extent this could lead to nonlinear effects in the derivation of the effective hydraulic properties, in particular the effective HCC. Furthermore, since the flow field for a given volume fraction of obstacles depends on dimensionality, i.e., is different in a 2D simulation than in a 3D simulation, studying the effects in the unsaturated region was one of the main motivations for performing this numerical analysis in 3D.

2.4. Inverse modeling of evaporation in 1D

A 10-day EVA experiment in 1D was simulated with the software package HYDRUS-1D (Šimůnek et al., 2006; 2008) to obtain the SHP parameters using inverse modeling. The generated data from the EVA and MSUG forward simulations in 3D were used as an input to the 1D inverse simulations. Time series of the pressure heads at three observation depths, mean volumetric water contents in the column during the virtual EVA experiment, and the data points of the effective HCC from the virtual MSUG experiment were used as data in the objective function. The time series of the mean volumetric water content was calculated from the initial water content, cumulative evaporation and soil volume. The measurement range for pressure heads used in the objective function was from saturation down to -2000 cm. This reflects a setup with laboratory tensiometers with boiling delay (Schindler et al., 2010). The time series of the simulated evaporation rates from the 3D simulations were used as the time variable atmospheric boundary condition for the 1D inverse simulations. The 1D soil profile was 10 cm long and was discretized into 100 equally sized finite elements. Similar to the 3D simulations, three observation points were defined in the depths of 2.5, 5.0 and 7.5 cm. A no-flux boundary condition was used at the bottom. The six parameters of the van Genuchten model occurring in Eq. (2) and (3) were all simultaneously estimated by inverse modeling. The weighted-least-squares objective function was minimized by the SCE-UA algorithm (Duan et al., 1992). The data obtained from the EVA experiment allow to identify the WRC from saturation to the pressure where the tensiometers fail, and the HCC in the mid to dry range of the SHP (roughly -100 to -2000 cm pressure head), while the MSUG provides a precise

187 determination of the HCC in the wet range (Sarkar et al., 2019; Durner and Iden, 2011). The EVA experiments do not
188 provide information on hydraulic conductivity near water-saturation (Peters et al., 2015). Therefore, we included the
189 obtained data from the virtual MSUG experiment in the object function for the inverse simulation of the virtual EVA
190 experiments, to improve the uniqueness of the inverse solution and the precision of the identified HCC near saturation
191 (see Schelle et al., 2010, for another example).

192 ### 2.5. Predicting SHP of virtual stony soils by scaling models

193 The SHP of stony soils obtained by inverse modeling were compared to SHP that are predicted by available scaling
194 models and used for their evaluation. Considering that f has the dominant influence on the WRC of a stony soil, a
195 common approach is partitioning the WRC and HCC of stony soil based on the volume of each component in the soil-
196 rock mixture and calculating the effective SHP of stony soil using the volume averaging or the composite-porosity
197 model. The general form of the WRC model considers the moisture contents of the background soil θ_{soil} (h) (cm^3 cm^{-3})
198 and embedded rock fragments θ_{rock} (h) (cm^3 cm^{-3}) to calculate the effective WRC of stony soils θ_m(h) (cm^3 cm^{-3})
199 (Flint and Childs, 1984; Peters and Klavetter, 1988) with the following form in the full moisture range (Naseri et al.,
200 2019):

$$\theta_m(h) = f\theta_{rock} + (1-f)\theta_{soil} \quad (4)$$

201 A typical assumption in stony soils hydrology is that the porosity of RF is negligible. In this case, Eq. (4) reduces to
202 (Bouwer and Rice, 1984):

$$\theta_m(h) = (1-f)\theta_{soil} \quad (5)$$

203 For the effective hydraulic conductivity of stony soils, some scaling models are developed for saturated conditions
204 that might apply to the hydraulic conductivity at any pressure heads. The simplest scaling model accounts only for the
205 reduction in the cross-sectional area available for flow of water. This leads to the equation (Ravina and Magier, 1984):

$$K_r = 1 - f \quad (6)$$

206 where K_r (-) is the relative hydraulic conductivity of stony soil, i.e., $K_r = K_m/K_{soil}$, where K_m is the effective hydraulic
207 conductivity of the stony soil (cm d^{-1}), and K_{soil} is the conductivity of the background soil (cm d^{-1}).

Ina more recent approach, Novák et al. (2011) developed a linear relationship based on the 2D numerical simulation results as a first approximation to scale the saturated hydraulic conductivity of stony soils:

$$K_{\mathrm{r}} = 1 - \alpha f \tag{7}$$

The parameter α was reported to depend on the texture of the background soil, with a range between 1.1 for sandy clay to 1.32 for clay. This model is easy to apply, but it requires the estimation of the parameter α to calculate K_{r}. For our calculations, we assumed $\alpha = 1.2$ for the sandy loam background soil used in our study.

Another model that has been developed for mixtures with spherical inclusions is the Maxwell model (Maxwell, 1873; Corring and Churchill, 1961; Peck and Watson, 1979; Zimmermann and Bodvarsson, 1995). It takes the value of f, hydraulic conductivity of the background soil and hydraulic conductivity of inclusions into account to calculate the hydraulic conductivity of the stony soil. In the special case of impermeable inclusions, Maxwell model reduces to:

$$K_{\mathrm{r}} = \frac{2(1-f)}{2+f} \tag{8}$$

A recently developed model by Naseri et al. (2020), which is based on the general effective medium theory (GEM), allows considering effects of permeability, shape, and orientation of RF on the effective HCC. For impermeable RF, the GEM model reduces to the following form:

$$K_{\mathrm{r}} = \left(1 - \frac{f}{f_{\mathrm{c}}}\right)^{t} \tag{9}$$

where f_{c} is the critical f with values between 0.84 and nearly 1 and t is a shape parameter with values between 1.26 and nearly 1.5 for spherical RF. In this study, we set $f_c = 0.982$ (v/v) according to the size ratio of the RF to the background soil, and $t = 1.473$ for spherical RF (for details, see appendix in Naseri et al., 2020).

It should be noted that all approaches apply at any pressure head h_i, i.e., the scaling that is originally developed for saturated conditions with locally constant hydraulic conductivity in the background soil is equally applied to unsaturated conditions.

3. Results and discussion

3.1. Flow field and variability of state variables in the virtual MSUG experiment

Figure 2 visualizes the pressure head (cm), water content ($cm^3\ cm^{-3}$), and velocity ($cm\ d^{-1}$) in a 2D cross section in the center of the soil column through the forward simulation of the MSUG experiment. The profile is shown for the steady state flux situation with a pressure head of -100 cm and the stony soil with f = 28.5 %. The Figure shows a considerable change in the flow velocities, even at the upper boundary. Also, as Fig. 2 illustrates, the conditions above an obstacle might be slightly wetter than below an obstacle, but the variations in the pressure head and the water content fields is very small. We note that this general finding was equally applicable for all other pressure heads steps in the virtual MSUG experiment.

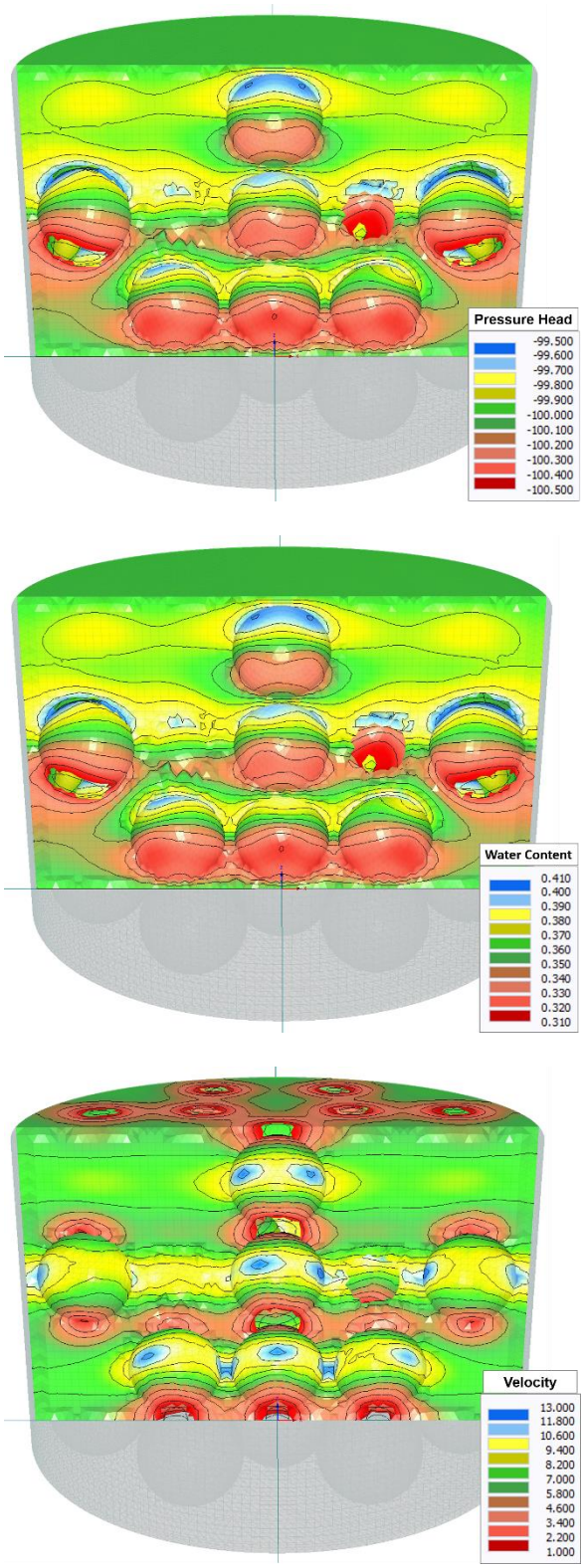

Figure 2: Visualization of the pressure head (cm), water content ($cm^3\ cm^{-3}$), and velocity ($cm\ d^{-1}$) in a 2D profile in the center of the soil column during the forward simulation of MSUG experiment.

3.2. Comparison of the relative K_s of the scaling models and the 3D simulations under saturated conditions

The dependency of the relative saturated hydraulic conductivity (K_r) on the percentage of RF, calculated by different scaling models and the obtained values from the first pressure in the virtual MSUG experiment is presented in Fig. 3. The results of the models are shown up to the $f = 37.3$ %, which was the highest value of f simulated in 3D. However, some of the evaluated models are theoretically valid for higher or lower values of f, e.g. 40 % for the Novák et al. (2011) model and higher values for the GEM model (Naseri et al., 2020).

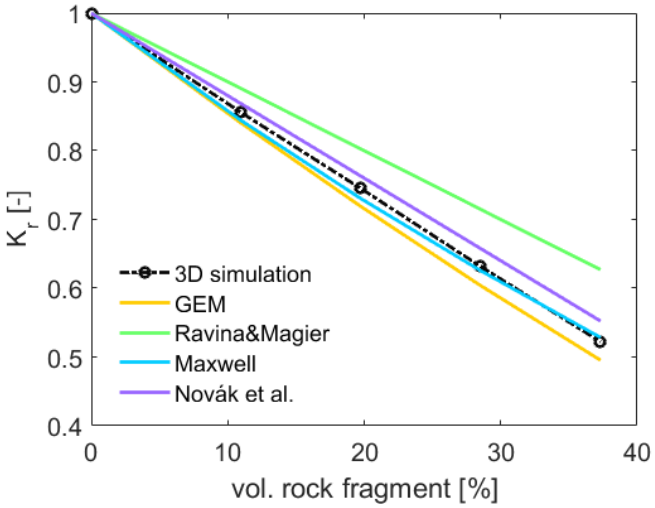

Figure 3: Comparison of the values of K_r (-) from the virtual MSUG experiment in 3D (circles), and calculated by different scaling models (solid lines) for f values up to 37.3 %. The dashed line connects the simulated data points of K_r shown by circles.

Obviously, the results of our simulations confirm a linear reduction of K_r with increasing the volume of RF up to $f = 37.3$ % (v/v) in the soil. The numerically obtained values of K_r are shown by circles and connected by the dashed line in Fig. 3. The dashed line has a slope of -1.29 representing a higher reduction rate of K_r compared to the scaling of K_r that would be proportional to f, expressed by Eq. (6) and predicted by the model of Ravina and Magier (1984) (solid green line). This result supports the fact that even in a stony soil with spherical impermeable RF, the reduction in the hydraulic conductivity is higher than the reduction of the average cross-sectional area (which is statistically equivalent to the value of f). Hlaváčiková et al. (2016) found an even higher value of -1.45 for spherical RF with a diameter of 10 cm. The model of Novák et al. (2011) performs better but also leads to a slight under-prediction of the reduction of the effective saturated conductivity. The performance of this model could be improved by adjusting the parameter α to match data of the 3D simulation, but doing this would lead to an unfair comparison with the other models. The two

models predicting a nonlinear relationship between the K_r and f, GEM and Maxwell, show similar results at low contents of RF up to 10 %, with minor differences in outputs of the models. Among all of the evaluated models of scaling K_s, the Maxwell model yields the closest match to the numerically identified values of K_r.

We note that these results may differ in natural soils, where an increase of the saturated hydraulic conductivity might be expected because of macropore flow in lacunar pores at the interface between background soil and RF (Beckers et al., 2016; Hlaváčiková et al., 2019, Arias et al., 2019). We have not included such a process in our 3D simulations.

3.3. Inverse modeling results for effective hydraulic properties

The observed and fitted time series of the pressure heads at the three representative observation points is shown in Fig. 4 for the simulated experiments of the four cases with different values of f. In each case, the fitted pressure heads at the three depths of the column (2.5, 5.0 and 7.5 cm) match well with the time series of the corresponding data from the 3D virtual experiments. Specifically, the match of the pressure heads at 7.5 and 5.0 cm is excellent, whereas there are slight systematic deviations at the uppermost level at the later stage of the virtual EVA experiment.

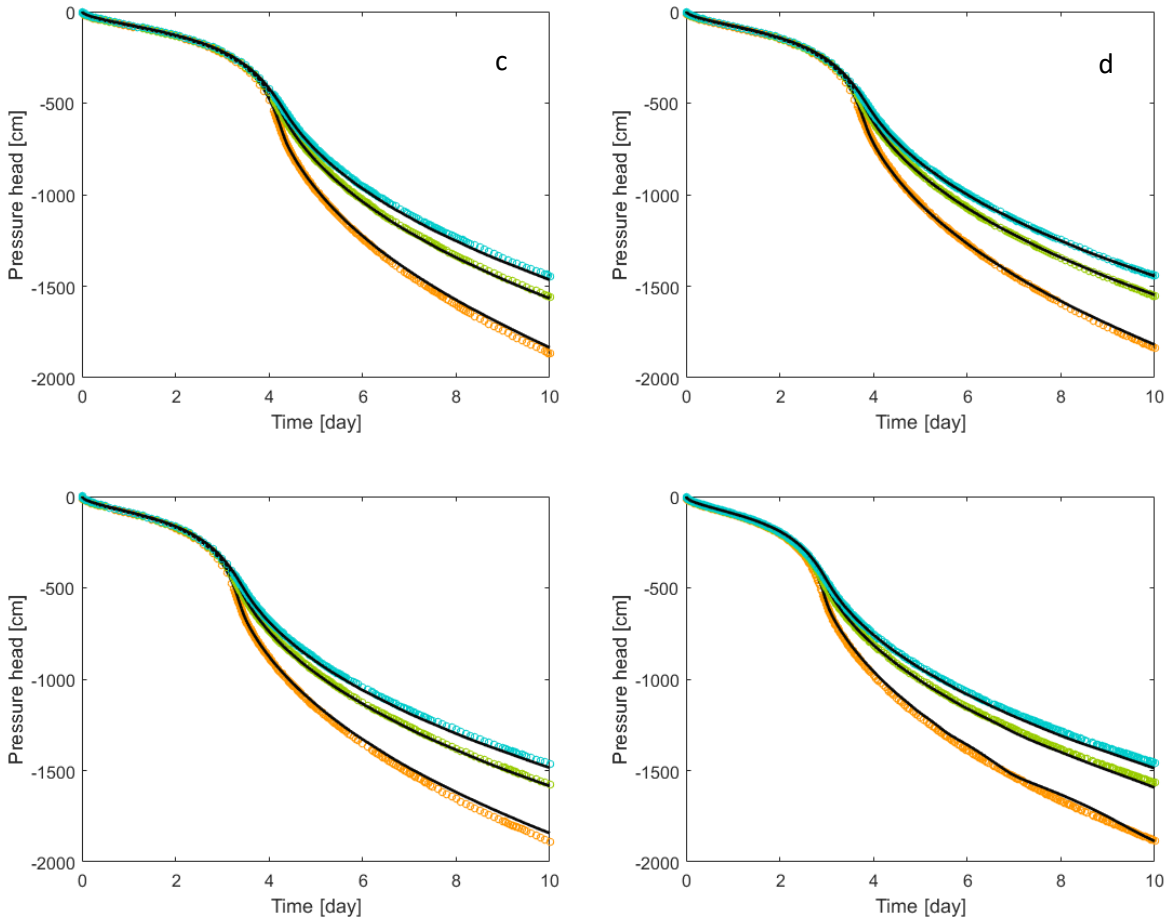

Figure 4: The time series of the 3D-simulated (circles) and 1D fitted (solid lines) pressure heads at the observation points in three depths of the stony soil columns with the f values a) 11.0 %, b) 19.8 %, c) 28.5 %, and d) 37.3 %. The observation depths are indicated by different color codes of orange (upper, 2.5 cm), green (middle, 5.0 cm) and blue (lower, 7.5 cm from top).

Table 1 shows the values of the root mean square error (RMSE) and mean absolute error (MAE) between the observed and fitted time series of the pressure heads at three observations points for values of f. According to the Table 1, the fit is best for the lower f and in the middle of the column. The highest deviations occur for the highest f but there is no clear trend. Overall, the values of RMSE and MAE are in an acceptable range regarding the observed values of pressure heads up to -2000 cm. This indicates that the time series of the pressure heads at multiple depths generated by the 3D simulations of EVA experiments can be described successfully by the 1D Richards equation assuming a homogenous system with effective SHP.

285 *Table 1: The values of RMSE and MAE between the observed and fitted pressure heads, in three observation points for different*
286 *values of f.*

Criteria	Observation point	Volumetric fraction of RF, f (%)			
		11.0	19.8	28.5	37.3
RMSE	upper	12.8	6.5	12.6	18.9
	middle	4.9	2.8	5.3	10.7
	lower	9.1	3.1	8.7	13.9
MAE	upper	10.0	4.9	9.4	14.5
	middle	4.0	2.1	4.5	8.5
	lower	7.0	2.6	6.8	11.0

287

288 The identified SHP are presented in Fig. 5. The solid lines in the Figure show the WRC and HCC of the virtual stony
289 soils obtained by inverse simulation (except the solid black lines, which are the WRC and HCC of the background
290 soil), the dashed lines represent the scaled WRC by Eq. (5) and HCC by Eq. (6), and the circles on the HCC plots
291 represent the discrete data points of hydraulic conductivity obtained by the virtual MSUG experiment. The WRC and
292 HCC are presented on a pF scale, which is defined as $pF = \log 10\,(|h|)$, in which h is the pressure head in cm
293 (Schofield, 1935). The van-Genuchten model parameters of the background soil and stony soils are shown in Table 2.

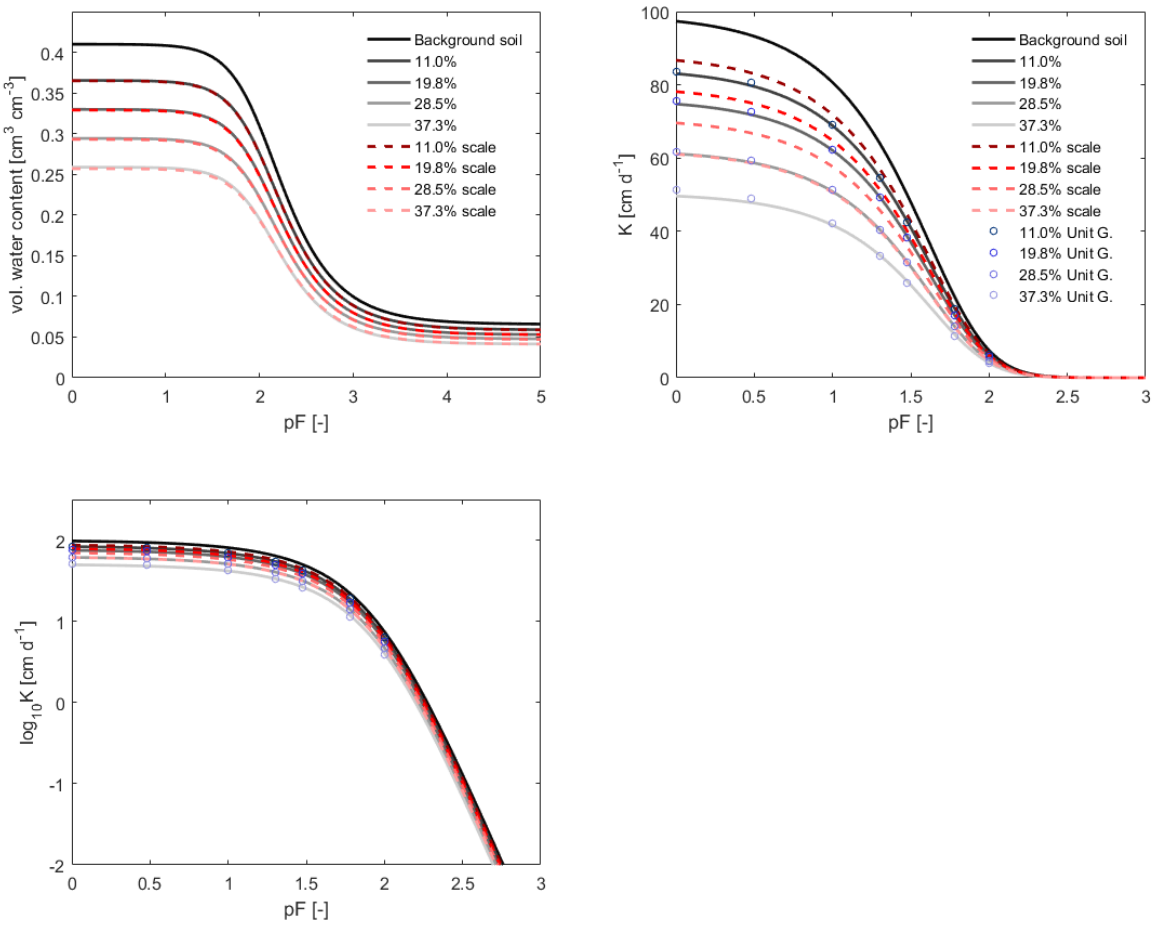

Figure 5: The WRC and HCC of the background soil (solid black line), and identified effective WRC (left) and HCC (right) of the virtual stony soils (solid gray lines) with different values of f. The HCC are presented also in the logarithmic scale. The dashed lines show the effective WRC and HCC calculated by the models of Bouwer and Rice (1984) and Ravina and Magier (1984). The circles on the HCC present the data points of hydraulic conductivity obtained by the virtual MSUG experiment in near-saturated conditions up to the $pF \approx 2$.

Table 2: The van-Genuchten model parameters of the SHP of the background soil and of the inversely determined effective SHP of the virtual stony soils with different values of f.

Parameter	Unit	Volumetric fraction of RF, f (%)				
		Background soil	11.0	19.8	28.5	37.3
θ_s	(cm^3 cm^{-3})	0.410	0.365	0.330	0.294	0.259
θ_r	(cm^3 cm^{-3})	0.065	0.059	0.053	0.048	0.041
α	(cm^{-1})	0.010	0.010	0.010	0.010	0.010
n	(-)	2.000	2.007	2.011	2.014	2.037
K_s	(cm d^{-1})	100.0	84.7	76.2	62.3	50.4
τ	(-)	0.50	0.43	0.47	0.42	0.38

According to the Fig. 5 and Table 2 the value of the shape parameter α is independent of the value of f and the change in the value of n is negligible (but might be systematic). The inversely identified WRC and the predictions from the Bouwer and Rice (1984) scaling model match almost perfectly for all the RF contents. In agreement with this, there is also an excellent agreement of the values of the saturated (θ_s) and residual water contents (θ_r) ($cm^3\ cm^{-3}$) between scaled and identified WRC. The values of θ_s and θ_r in the WRC are directly related to the values of f and the respective values of the background soil and the WRC is scaled by this factor over the whole range of soil water pressure head.

Similar to the WRC, an increase of f reduces the hydraulic conductivity over the whole range of pressure head covered by the virtual experiments. However, in contrast to the WRC, the simple scaling model based on Eq. (6) cannot describe the reduction in HCC. Figure 5 shows that the model of Ravina and Magier (1984, dashed lines) underestimates the reduction of the effective HCC for all rock contents. The reason might be related to the local variations of the flow velocity in the soil column. It was shown in Fig. 2 that the variations in the water flow velocity might be considerable. The nonlinearities in the flow field and changes in the local conductivities, together with an increased average flow path length, force a stronger overall conductivity reduction. The arrangement of RF thus might affect the reduction in hydraulic conductivities, leading to different conductivities at the same value of f (Naseri et al., 2020). The degree depends on how the flow area is altered in the soil column due to the presence of RF (Fig. 1 and 2). This result is in agreement with Novák et al. (2011) who reported a higher reduction in conductivity compared to a reduction that is proportional to the rock fragments content. Furthermore, it may also differ alter depending on the characteristics of RF such as their size, shape and orientation towards flow (Novák et al., 2011).

We had to include the data points of hydraulic conductivity from the virtual MSUG experiment in the inverse objective function to get a precise identification of the HCC obtained by inverse modeling near saturation. The information content from the virtual EVA experiment gives a unique identification only when the flux rate in the system reaches the magnitude of the unsaturated hydraulic conductivity, which is for many soils around $pF = 1.5$ to $pF = 2$ (Peters and Durner, 2008). Although there are some discrepancies visible near saturation for the case with a high value of f, the resulting values of hydraulic conductivity from the virtual MSUG experiment and the inversely identified HCC using the virtual EVA experiment join well around $pF = 2$ for all of the values of f. Therefore, the HCC could be described successfully from the saturation up to $pF = 3$ using the inverse modeling of the virtual EVA experiment with added K support points from the virtual MSUG experiment. The overall results suggest that the effective

hydraulic parameters of stony soils could be obtained by the corresponding real experiments and the result is robust for both, WRC an HCC, even if the uncertainty in the identified HCC is higher than that of the WRC (Singh et al., 2020; 2021).

3.4. Evaluation of the Novák, Maxwell and GEM models using the identified HCC

As stated above, the model of Ravina and Magier (1984) which is a linear scaling approach of the hydraulic conductivity (Eq. 6) underestimates the reduction of conductivity in the stony soil. We used the identified HCC as a benchmark to evaluate and compare more advanced models of scaling HCC, namely the Novák, Maxwell and GEM models (Eq. 7, 8 and 9). Figure. 6 illustrates the calculated HCC of stony soils with different values of f using these models of scaling HCC and compares them to the identified HCC by the inverse modeling.

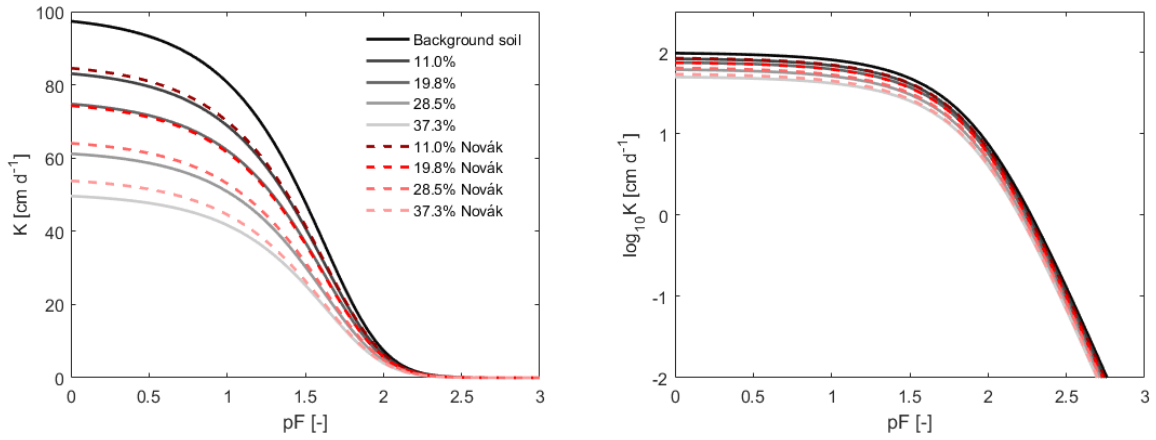

341

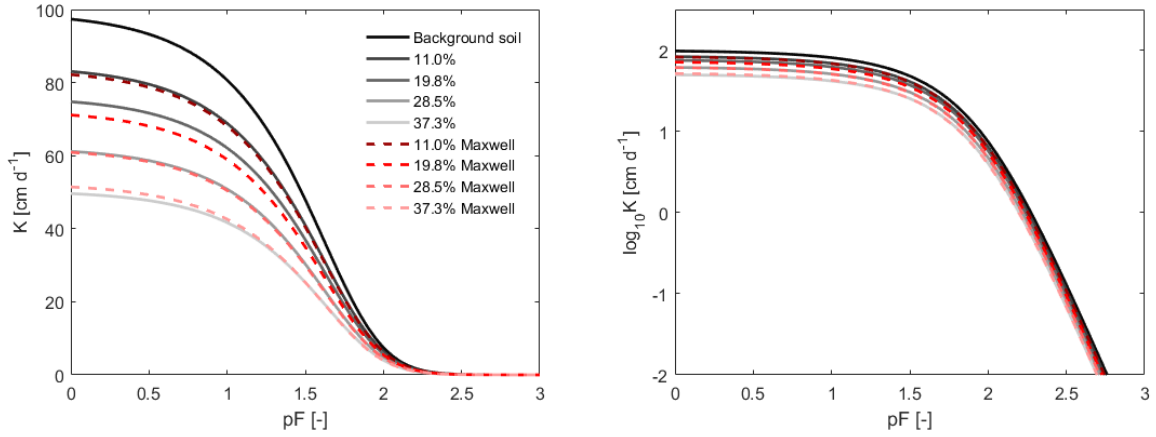

342

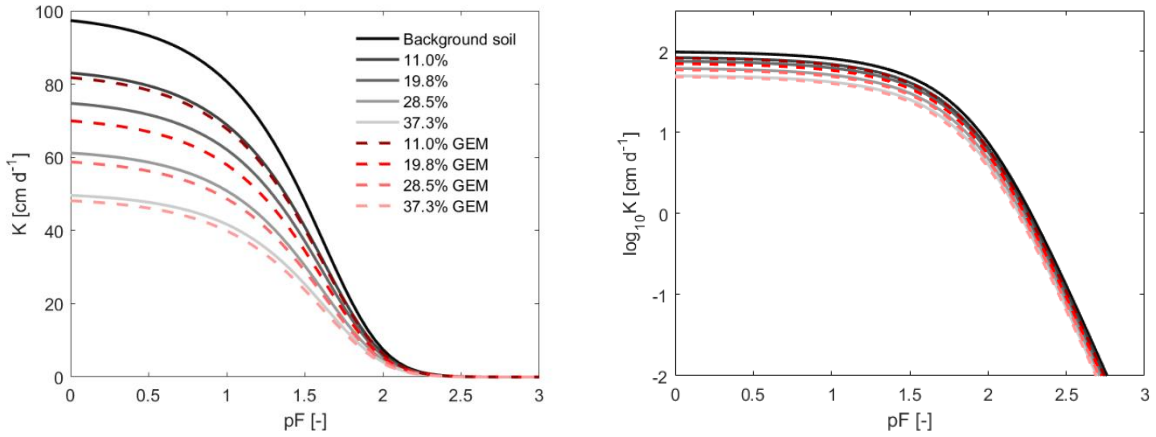

343

344 *Figure 6: Evaluation of the Novák, Maxwell and GEM models of scaling HCC of stony soils using the identified HCC as a*
345 *benchmark. The HCC in each case were obtained for f=11.0, 19.8, 28.5 and 37.3 % (v/v). The inverse identified curves are shown*
346 *in solid lines and the model results in dashed lines. The value of f_c in the GEM model was set as 0.982 with the corresponding*
347 *shape parameter t=1.473 and the parameter $\alpha = 1.2$ was selected for the Novák model.*

348

The calculated HCC by the three models are in general in good agreement with the identified HCC in the observed range of pressure heads. All three models result in a more realistic estimate of the HCC compared to the simple linear scaling approach. While the model of Novák slightly underestimates the identified HCC for all the four RF contents, the results are contrary for the GEM model where the reduction in the hydraulic conductivity is overestimated. The Maxwell model shows the same results as GEM model except for the stony soil with $f = 37.3$ % where it underestimates the HCC.

In order to compare the performance of the three models, the average deviation (d_{avg}) between the calculated and identified HCC (logarithmic scale) was calculated to quantify the error of each model in the pF range 0 to 3 (Table 3). The signs of numbers in Table 3 represent the tendency of the model in over- or underestimating the identified hydraulic conductivities. The negative sign means the model underestimates the reduction of hydraulic conductivity.

Table 3: Performance of the Novák, Maxwell and GEM models quantified by the average deviation of log10 (K) (d_{avg}) for different values of f.

model	Volumetric fraction of RF, f (%)			
	11.0	19.8	28.5	37.3
Novák	-0.0068	-0.0028	-0.0179	-0.0231
Maxwell	0.0056	0.0162	0.0039	-0.0038
GEM	0.0077	0.0234	0.0197	0.0248

Table 3 confirms the qualitative tendency of underestimation of the conductivity reduction by the Novák model and the overestimation by the GEM and Maxwell models, but also shows that the difference between the three models is not large and probably not of relevance in practice (the GEM model at the high value of f, which has the highest deviation, corresponds to a relative mismatch of K of 6 %). However, despite the potential of the three models in predicting the HCC of stony soils, we think they require further evaluations using field measured data of hydraulic conductivity in different experimental conditions.

4. Conclusions

In this study, we created virtual stony soils with different volumetric fractions of RF in 3D and identified their effective SHP from saturation up to $pF = 3$ by inverse modeling of virtual EVA and MSUG experiments in 1D. We used the identified SHP to investigate the performance of the available scaling models in stony soils, namely the Bouwer and

Rice (1984) model of scaling the WRC, and Ravina and Magier (1984), Maxwell (Peck and Watson, 1979), Novák (Novák et al., 2011), and GEM (Naseri et al., 2020) models for scaling HCC of stony soils.

Our results show that the boundary fluxes and the internal system states in the virtual 3D EVA experiments, represented by the observed time series of pressure heads at multiple depths, could be matched well by 1D simulations, and the effective WRC and HCC of the considered stony soils were determined accurately. Comparison with the scaling models showed that by assuming a homogeneous background soil and impermeable RF, the effective WRC can be calculated from the WRC of the background soil using a simple correction factor equal to the volume fraction of background soil, $(1-f)$. That is a result with practical implications in obtaining WRC of stony soils. In addition, the scaling results for HCC were promising. Our results confirmed that the reduction in K_r was stronger than calculated by a simple proportionality to $(1-f)$. The three models of Novák, Maxwell, and GEM consider that and performed adequately in predicting the effective HCC of stony soils. The Maxwell model matched the numerical results best.

Care must be taken before generalizing these results to arbitrary conditions, e.g., highly dynamic boundary conditions with sequences of precipitation and higher and lower evaporation rates, which might yield different results due to the occurrence of non-equilibrium water dynamics and hysteresis. For real stony soils, changes in the pore size distribution of the background soil may result from the presence of RF (Sekucia et al., 2020) with corresponding consequences for effective SHP. This influence was reported to be more common in compactable soils with a shrinkage-swelling potential (Fiès et al., 2002). In highly stony soils, where RF are not embedded completely in the background soil, the existence of effective SHP is still an open question. Finally, the impact of arrangement and size of RF on evaporation dynamics and effective SHP needs to be understood. Tackling these problems requires a combination of experimental and modelling approaches.

References

Abbasi, F., Jacques, D., Šimůnek, J., Feyen, J., and Van Genuchten, M.T.: Inverse estimation of soil hydraulic and solute transport parameters from transient field experiments: Heterogeneous soil, Transactions of the ASAE, 46(4), 1097, doi: 10.13031/2013.13961, 2003.

Arias, N., Virto, I., Enrique, A., Bescansa, P., Walton, R., and Wendroth, O.: Effect of Stoniness on the Hydraulic Properties of a Soil from an Evaporation Experiment Using the Wind and Inverse Estimation Methods, Water, 11(3), 440, doi: 10.3390/w11030440, 2019.

Ballabio, C., Panagos, P., and Monatanarella, L.: Mapping topsoil physical properties at European scale using the LUCAS database, Geoderma, 261, 110-123, doi: 10.1016/j.geoderma.2015.07.006, 2016.

401 Beckers, E., Pichault, M., Pansak, W., Degré, A., and Garré, S.: Characterization of stony soils´ hydraulic conductivity
402 using laboratory and numerical experiments, Soil, 2, 421– 431, doi: 10.5194/soil-2-421-2016, 2016.

403 Bouwer, H., and Rice, R.C.: Hydraulic properties of stony vadose zones, Ground Water, 22, 696–705, doi:
404 10.1111/j.1745-6584.1984.tb01438.x, 1984.

405 Brakensiek, D.L., Rawls, W.J., and Stephenson, G.R.: Determining the saturated conductivity of a soil containing rock
406 fragments, Soil Sci. Soc. Am. J., 50, 834-835, doi: 10.2136/sssaj1986.03615995005000030053x, 1986.

407 Celia, M.A., Bouloutas, E.T. and Zarba, R.L.: A general mass-conservative numerical solution for the unsaturated
408 flow equation, Water Resour. Res., 26(7), 1483-1496, doi: 10.1029/WR026i007p01483, 1990.

409 Coppola, A., Dragonetti, G., Comegna, A., Lamaddalena, N., Caushi, B., Haikal, M.A., and Basile, A.: Measuring
410 and modeling water content in stony soils, Soil Till. Res., 128, 9-22, doi: 10.1016/j.still.2012.10.006, 2013.

411 Corwin, D.L., and Lesch, S.M.: Apparent soil electrical conductivity measurements in agriculture, Comput. Electron.
412 Agr., 46 (1-3), 11-43, doi: 10.1016/j.compag.2004.10.005, 2005.

413 Cousin, I., Nicoullaud, B., and Coutadeur, C.: Influence of rock fragments on the water retention and water percolation
414 in a calcareous soil, Catena, 53: 97–114, doi: 10.1016/S0341-8162(03)00037-7, 2003.

415 Dann, R., Close, M., Flintoft, M., Hector, R., Barlow, H., Thomas, S., and Francis, G.: Characterization and estimation
416 of hydraulic properties in an alluvial gravel vadose zone, Vadose Zone J., 8(3), 651-663, doi: 10.2136/vzj2008.0174,
417 2009.

418 Durner, W., and Flühler, H.: Chapter 74: Soil hydraulic properties, in M. G. Anderson, and J. J. McDonnell (Eds.), in:
419 Encyclopedia of hydrological sciences, chapter 74, 1103–1120. John Wiley & Sons.,
420 doi:10.1002/0470848944.hsa077c, 2006.

421 Durner, W., and Iden, S.C.: Extended multistep outflow method for the accurate determination of soil hydraulic
422 properties near water saturation, Water Resour. Res., 47(8), doi: 10.1029/2011WR010632, 2011.

423 Durner, W., Jansen, U., and Iden, S.C.: Effective hydraulic properties of layered soils at the lysimeter scale determined
424 by inverse modelling, Euro. J. Soil Sci., 59(1), 114-124, doi: 10.1111/j.1365-2389.2007.00972.x, 2008.

425 Farthing, M.W., and Ogden, F.L.: Numerical solution of Richards' equation: A review of advances and challenges,
426 Soil Sci. Soc. Am. J., 81(6), 1257-1269, doi: 10.2136/sssaj2017.02.0058, 2017.

427 Fiès, J.C., Louvigny, N.D.E., and Chanzy, A.: The role of stones in soil water retention, Euro. J. Soil Sci., 53(1), 95-
428 104, doi: 10.1046/j.1365-2389.2002.00431.x, 2002.

429 Germer, K., and Braun J.: Determination of anisotropic saturated hydraulic conductivity of a macroporous slope soil,
430 Soil Sci. Soc. Am. J., 79, 1528-1536, doi: 10.2136/sssaj2015.02.0071, 2015.

431 Grath, S.M., Ratej, J., Jovičić, V., and Curk, B.: Hydraulic characteristics of alluvial gravels for different particle sizes
432 and pressure heads, Vadose Zone J., 14 (3), doi: 10.2136/vzj2014.08.0112, 2015.

433 Haghverdi, A., Öztürk, H.S., and Durner, W.: Measurement and estimation of the soil water retention curve using the
434 evaporation method and the pseudo continuous pedotransfer function, J. hydrol., 563, 251-259, doi:
435 10.1016/j.jhydrol.2018.06.007, 2018.

436 Hlaváčiková, H., and Novák V.: A relatively simple scaling method for describing the unsaturated hydraulic functions
437 of stony soils, J. Plant Nutr. Soil Sci., 177, 560–565, doi: 10.1002/jpln.201300524, 2014.

438 Hlaváčiková, H., Novák V., and Šimůnek J.: The effects of rock fragment shapes and positions on modeled hydraulic
439 conductivities of stony soils, Geoderma, 281, 39–48, doi: 10.1016/j.geoderma.2016.06.034, 2016.

Hlaváčiková, H., Novák, V., Kostka, Z., Danko, M., and Hlavčo, J.: The influence of stony soil properties on water dynamics modeled by the HYDRUS model, J. Hydrol. Hydromech., 66(2), 181-188, doi: 10.1515/johh-2017-0052, 2018.

Hopmans J.W., Šimůnek J., Romano N., and Durner W.: Inverse Modeling of Transient Water Flow, in: Methods of Soil Analysis, Part 1, Physical Methods, Chapter 3.6.2, Eds. J. H. Dane and G. C. Topp, Third edition, SSSA, Madison, WI, 963–1008, 2002.

Kutilek, M.: Soil hydraulic properties as related to soil structure, Soil and Tillage Research, 79(2), 175-184, doi: 10.1016/j.still.2004.07.006, 2004.

Lai, J., and Ren, L.: Estimation of effective hydraulic parameters in heterogeneous soils at field scale, Geoderma, 264, 28-41, doi: 10.1016/j.geoderma.2015.09.013, 2016.

Lehmann, P., Bickel, S., Wei, Z., and Or, D.: Physical constraints for improved soil hydraulic parameter estimation by pedotransfer functions, Water Resour. Res., 56(4), e2019WR025963, doi: 10.1029/2019WR025963, 2020.

Mualem, Y.: A new model for predicting the hydraulic conductivity of unsaturated porous media, Water Resour. Res., 12, 513–521, doi: 10.1029/WR012i003p00513, 1976.

Naseri, M., Iden, S. C., Richter, N., and Durner, W.: Influence of stone content on soil hydraulic properties: experimental investigation and test of existing model concepts, Vadose Zone J., 18(1), 1-10., doi: 10.2136/vzj2018.08.0163, 2019.

Naseri, M., Peters, A., Durner, W., and Iden, S.C.: Effective hydraulic conductivity of stony soils: General effective medium theory, Adv. Water Resour., 146, 103765, doi: 10.1016/j.advwatres.2020.103765, 2020.

Nasta, P., Huynh, S., and Hopmans, J.W.: Simplified multistep outflow method to estimate unsaturated hydraulic functions for coarse-textured soils, Soil Sci. Soc. Am. J., 75(2), 418-425, doi: 10.2136/sssaj2010.0113, 2011.

Novák, V., and Hlaváčiková, H.: Applied Soil Hydrology, Springer International Publishing, doi: 10.1007/978-3-030-01806, 2019.

Novák, V., Kňava, K., and Šimůnek, J.: Determining the influence of stones on hydraulic conductivity of saturated soils using numerical method, Geoderma, 161, 177–181. doi: 10.1016/j.geoderma.2010.12.016, 2011.

Peters, A., and Durner, W.: Simplified evaporation method for determining soil hydraulic properties, J. Hydrol., 356 (1-2), 147-162, doi: 10.1016/j.jhydrol.2008.04.016, 2008.

Peters, A., Iden, S.C., and Durner, W.: Revisiting the simplified evaporation method: Identification of hydraulic functions considering vapor, film and corner flow, J. Hydrol., 527, 531-542, doi: 10.1016/j.jhydrol.2015.05.020, 2015.

Peters, R. R., and Klavetter, E. A.: A continuum model for water movement in an unsaturated fractured rock mass, Water Resour. Res., 24, 416–430, doi: 10.1029/WR024i003p00416, 1988.

Ponder, F., and Alley, D.E.: Soil sampler for rocky soils. US Department of Agriculture, Forest Service, North Central Forest Experiment Station, 1997.

Radcliffe, D.E., and Šimůnek, J.: Soil physics with HYDRUS: Modeling and applications. CRC press, 2018.

Ravina, I., and Magier, J.: Hydraulic conductivity and water retention of clay soils containing coarse fragments, Soil Sci. Soc. Am. J., 48(4), 736-740., doi: 10.2136/sssaj1984.03615995004800040008x, 1984.

Russo, D.: Determining soil hydraulic properties by parameter estimation: On the selection of a model for the hydraulic properties, Water Resour. Res., 24(3), 453-459, doi: 10.1029/WR024i003p00453, 1988.

Sarkar, S., Germer, K., Maity, R., and Durner, W.: Measuring near-saturated hydraulic conductivity of soils by quasi unit-gradient percolation—1. Theory and numerical analysis, J. Plant Nutr. Soil Sc., 182(4), 524-534, doi: 10.1002/jpln.201800382, 2019.

Schelle, H., Iden, S.C., Peters, A., and Durner, W.: Analysis of the agreement of soil hydraulic properties obtained from multistep-outflow and evaporation methods, Vadose Zone J., 9(4), 1080-1091, doi: 10.2136/vzj2010.0050, 2010.

Schelle, H., Durner, W., Schlüter, H., Vogel, H.-J., and Vanderborght, J.: Virtual Soils: Moisture measurements and their interpretation by inverse modeling, Vadose Zone J., 12:3, doi: 10.2136/vzj2012.0168, 2013.

Schindler, U., Durner, W., von Unold, G., and Müller, L.: Evaporation method for measuring unsaturated hydraulic properties of soils: Extending the measurement range, Soil Sci. Soc. Am. J., 74(4), 1071-1083, doi: 10.2136/sssaj2008.0358, 2010.

Schofield, R.K.: The pF of water in soil, in: Trans. of the Third International Congress on Soil Science, 2, Plenary Session Papers, 30 July-7 August, 1935 Oxford, UK, pp. 37-48, 1935.

Sekucia, F., Dlapa, P., Kollár, J., Cerdá, A., Hrabovský, A., and Svobodová, L.: Land-use impact on porosity and water retention of soils rich in rock fragments, CATENA, 195, 104807, doi: 10.1016/j.catena.2020.104807, 2020.

Šimůnek, J., Van Genuchten, M.T., and Šejna, M.: The HYDRUS software package for simulating two-and three-dimensional movement of water, heat, and multiple solutes in variably-saturated media, Technical manual, version, 1, 241, 2006.

Šimůnek, J., van Genuchten, M.T., and Šejna, M.: Development and applications of the HYDRUS and STANMOD software packages and related codes, Vadose Zone J., 7(2), 587-600, doi: 10.2136/vzj2007.0077, 2008.

Šimůnek, J., Van Genuchten, M.T., and Šejna, M.: Recent developments and applications of the HYDRUS computer software packages, Vadose Zone J., 15(7), doi: 10.2136/vzj2016.04.0033, 2016.

Singh, A., Haghverdi, A., Öztürk, H.S., and Durner, W.: Developing Pseudo Continuous Pedotransfer Functions for International Soils Measured with the Evaporation Method and the HYPROP System: I. The Soil Water Retention Curve, Water, 12(12), 3425, doi: 10.3390/w12123425, 2020.

Singh, A., Haghverdi, A., Öztürk, H.S., and Durner, W.: Developing Pseudo Continuous Pedotransfer Functions for International Soils Measured with the Evaporation Method and the HYPROP System: II. The Soil Hydraulic Conductivity Curve, Water, 13(6), 878, doi: 10.3390/w13060878, 2021.

Stevenson, M., Kumpan, M., Feichtinger, F., Scheidl, A., Eder, A., Durner W., and Strauss, P.: Innovative method for installing soil moisture probes in a large-scale undisturbed gravel lysimeter, Vadose Zone J., 1–7, doi: 10.1002/vzj2.20106, 2021.

Tetegan, M., de Forges, A.R., Verbeque, B., Nicoullaud, B., Desbourdes, C., Bouthier, A., Arrouays, D., and Cousin, I.: The effect of soil stoniness on the estimation of water retention properties of soils: A case study from central France, Catena, 129, 95-102, doi: 10.1016/j.catena.2015.03.008, 2015.

Van Genuchten, M.T.: A closed-form equation for predicting the hydraulic conductivity of unsaturated soils, Soil Sci. Soc. Am. J., 44, 892-898, doi: 10.2136/sssaj1980.03615995004400050002x, 1980.

Verbist, K.M.J., Cornelis, W.M., Torfs, S., and Gabriels, D.: Comparing methods to determine hydraulic conductivities on stony soils, Soil Sci. Soc. Am. J., 77(1), 25-42, doi: 10.2136/sssaj2012.0025, 2013.

Wang, W., Sun, L., Wang, Y., Wang, Y., Yu, P., Xiong, W., Shafeeque, M., and Luo, Y.: A convex distribution of vegetation along a stony soil slope due to subsurface flow in the semiarid Loess Plateau, northwest China, J. Hydrol., 586, 124861, doi: 10.1016/j.jhydrol.2020.124861, 2020.

Zhang, Y., Zhang, M., Niu, J., Li, H., Xiao, R., Zheng, H., and Bech, J.: Rock fragments and soil hydrological processes: significance and progress, Catena, 147, 153-166, doi: 10.1016/j.catena.2016.07.012, 2016.

Zimmerman, R. W., and Bodvarsson, G.S.: The effect of rock fragments on the hydraulic properties of soils. Lawrence Berkeley Lab., CA, USA, USDOE, Washington, D.C., USA, doi: 10.2172/102527, 1995.